Absence of spin transport in the organic semiconductor Alq_3

J. S. Jiang, J. E. Pearson, and S. D. Bader
Materials Science Division, Argonne National Laboratory, Argonne, Illinois 60439, USA
(Received 16 July 2007; published 2 January 2008)

There have been differing interpretations regarding the magnetoresistance (MR) reported in spin-valve structures containing thick layers of the organic semiconductor tris-(8-hydroxyquinoline) aluminum (Alq_3). While some attribute it to spin injection and transport in Alq_3, others suggest tunneling through locally thin regions of the Alq_3 layer as the mechanism. We present results of magnetotransport and charge transport measurements on Alq_3-based spin valves and unipolar devices where the Alq_3 thickness is beyond the tunneling limit. We observe no measurable MR in the $Fe/Alq_3/Co$ spin valve structures. Measurements of temperature-dependent current-voltage characteristics and comparisons with unipolar devices show that charge transport in $Fe/Alq_3/Co$ spin valves is by holes only and is injection-limited. The hole-only transport in Alq_3 is stable only at low current densities. This supports the tunneling interpretation of the earlier reported MR. Similar to inorganic semiconductors, the large conductivity mismatch between the metal electrodes and the organic semiconductor prevents spin injection. However, inserting a tunnel barrier between the magnetic electrode and the organic semiconductor did not improve spin injection.

DOI: 10.1103/PhysRevB.77.035303 PACS number(s): 85.75.−d, 72.80.Le, 72.25.Dc, 72.25.Hg

I. INTRODUCTION

Harnessing the spin degree of freedom in electronic transport has given rise to the new field of spintronics, where metallic spin valves based on the giant magnetoresistance (GMR) and tunnel magnetoresistance (TMR) effects have already transformed information storage. Spin manipulation in semiconductors inspires the vision of merging electronics, magnetics, and photonics for multifunctional devices and ultimately, quantum computing in the solid state.[1] Organic materials are considered to be another promising medium for spin transport because the weak spin-orbit and hyperfine interactions result in long spin relaxation times.[2] Coherent spin transfer and spin-dependent transport have been demonstrated in molecular bridges and tunnel barriers.[3,4] Organic electronics is a burgeoning field, providing low-cost alternatives to electronic and photonic devices such as light emitting diodes, field effect transistors, and photovoltaic cells that are presently the domain of conventional inorganic semiconductors.[5] The prospect of applying spintronic principles to organic electronics is alluring. For example, Davis and Bussmann[6] pointed out that injecting spin-polarized electrons and holes simultaneously into an organic light emitting diode (OLED) would alter the population ratio of the emissive singlet excitons to the nonemissive triplet excitons, leading to a "magnetoluminescence" effect where the luminescence yield varies with the relative magnetic alignment of the electrodes and could be used to improve the efficiency of OLED devices.

The recent reports of a GMR effect in organic spin valve structures[7–11] are a significant development. These spin valves contain metallic or half-metallic ferromagnetic electrodes connected laterally or vertically by a layer of π-conjugated organic semiconductors. One of the organic materials is tris-(8-hydroxyquinoline) aluminum (Alq_3), an archetypal electroluminescent organic semiconductor used in OLEDs. The MR in these structures is quite large and is temperature- and bias-dependent, reaching a few tens percent at low temperatures. This is in contrast to inorganic semiconductors where all-electric spin injection and detection via metal electrodes have shown effects of $<1\%$ and are difficult to distinguish from stray-field-induced Hall effect or magnetoresistance contributions.[12,13] More importantly, the organic spacers in these spin valves have thicknesses (or width, in the case of lateral structures[7]) that are a few tens to more than 100 nm. At such distances, tunneling is not a viable conduction mechanism. It was proposed that spin-polarized charge carriers are injected from one ferromagnetic electrode into the organic spacer, where they drift through the organic spacer under the influence of the electric field and are collected at the opposite ferromagnetic electrode, giving rise to the GMR effect.[8–11] Assuming an exponential decay of the spin polarization, the spin diffusion length in Alq_3 was determined to be 45 nm at 11 K.[8] It is curious that in these structures, significant conduction occurs at very low bias voltages (tens of mV), whereas organic electronic devices with comparable organic layer thicknesses typically require several volts to operate.

That spins are being transported in organic materials by processes other than tunneling necessarily means that they occupy the molecular levels and participate in molecular electronic processes. It is natural to expect that spin-polarized conduction in OLEDs would lead to an observable magnetoluminescence effect. Salis *et al.*[14] fabricated Alq_3-based OLEDs with ferromagnetic electrodes and observed changes in the electroluminescence when the magnetization directions of the electrodes were switched. However, they recognized that this hysteretic electroluminescence was the result of stray fields from the magnetic electrodes rather than due to spin-polarized transport because the same effect also occurred in OLEDs having only one magnetic electrode. They deduced an upper limit of 5×10^{-5} for spin polarization due to injection. More recently, Xu *et al.*[15] observed transport behaviors consistent with tunneling in their organic spin valves having relatively thick (10–20 nm) Alq_3 spacers. Recalling the large roughness in their organic layers, they sug-

gest that tunneling through locally thin regions is the transport mechanism for their observed MR. Spin-polarized tunneling through ultrathin (monolayer level) Alq_3 layers into superconductors has also been reported by Santos *et al.*[16] Taken together, these reports prompt questions about the earlier interpretation that the magnetoresistance in organic spin valves is a GMR effect: Can spin-polarized carriers indeed be injected into and transported across Alq_3 at the molecular levels? And is magnetic control of not just conduction, but also other electronic and photonic properties, possible in Alq_3-based devices?

Although the conduction process in organic semiconductors is generally understood as being field-assisted thermionic injection followed by site-to-site hopping of electrons and holes, a large number of chemical, structural and morphological factors affect electronic transport in realistic organic devices.[17] In the case of organic spin valves and magnetic OLEDs, differences in the devices fabricated by different groups are likely to exist, and local characterizations might not have captured the extrinsic factors that actually determine the device characteristics. Therefore the debate over spin-polarization in these structures is best viewed from the questions of what the spin-bearing charge carriers are, and how they are being injected across the ferromagnet-organic interface and transported across the organic layer.

In this paper, we present details of device fabrication and transport measurements on Alq_3-based spin valves and unipolar devices where the Alq_3 thickness is beyond the tunneling limit. We observe no measurable MR in our $Fe/Alq_3/Co$ spin valve structures. We examine the nature of charge transport in $Fe/Alq_3/Co$ spin valves by measuring the temperature-dependent current density-voltage (J-V) characteristics and compare with unipolar devices. We find that charge transport in $Fe/Alq_3/Co$ spin valves is by holes only; the hole-only transport in Alq_3 is stable only at low current densities and is injection-limited. That the hole-only transport in $Fe/Alq_3/Co$ spin valves cannot sustain the high current densities as used in earlier studies supports the interpretation of tunneling as the mechanism for the MR in those reports. The lack of MR in our $Fe/Alq_3/Co$ spin valve is similar to the case of a ferromagnetic metal-inorganic semiconductor interface, where the "conductivity mismatch problem" prevents efficient spin injection.[18] However, inserting a tunnel barrier between the magnetic electrode and the organic semiconductor did not improve spin injection. This suggests possible intrinsic spin-depolarizing hole transport in Alq_3.

II. EXPERIMENTAL DETAILS

Our devices are in the standard cross configuration. The top and bottom metal electrodes are patterned rectangular strips perpendicular to each other, and the Alq_3 organic layer is sandwiched in-between. The overlap of the electrodes defines the active area of a device. The electrode materials for the spin valve structures are Fe and Co. To ensure that we obtain distinct parallel and antiparallel magnetic configurations, the Co electrode is exchange-coupled to a 5-nm-thick layer of reactively sputtered CoO in order to increase its coercivity. The tunnel barrier was aluminum oxide (AlO_x). For the unipolar devices, we replaced the Fe electrode of the spin valves with Mg or Au. Mg and Au are the common electron- and hole-injecting materials, respectively, for organic electronics. Figure 1 compares the work functions of the metals[19] and the highest occupied molecular orbital (HOMO) and the lowest unoccupied molecular orbital (LUMO) levels of Alq_3.[20] The interface dipoles at the metal/Alq_3 interface often give rise to a vacuum level offset, which generally lowers the molecular levels of Alq_3. The typical value of the vacuum level offset for the metal-Alq_3 pairs used here is $\sim$1 eV.[21,22] This makes the energy barrier for Mg to inject electrons into $Alq_3 \sim 1.46$ eV, and that for hole injection by Au ~ 1.7 eV.

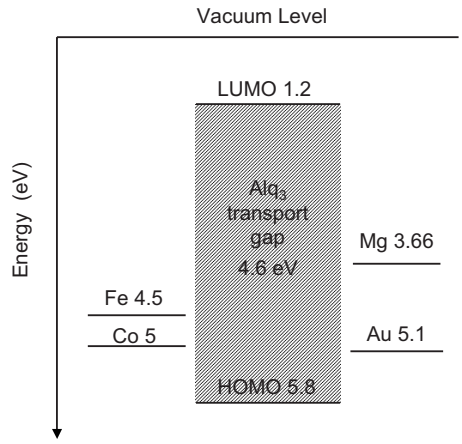

FIG. 1. Schematic energy-level diagram showing the Alq_3 molecular levels and the work functions of the metal electrodes. The vacuum level is depicted as a common reference here. However, there generally exists a vacuum level offset at the metal-Alq_3 interface, lowering the molecular levels of Alq_3.

We prepared our samples in a high-vacuum deposition system containing interconnected growth chambers for metal and organic materials. The system base pressure was $<2 \times 10^{-8}$ Torr. The substrates were SiN-coated Si wafers. The electrodes were defined by shadow masks having single or multiple parallel slits. Various slit widths were used, resulting in device areas ranging from 2×2 mm^2 to 100×100 μm^2. The Alq_3 layer was unpatterned, covering the entire substrate and the bottom electrode. The sample transfer and mask changing between deposition steps were performed without breaking vacuum, ensuring clean interfaces between the layers. On each substrate, a set of up to seven nominally identical devices was made. All electrodes had a thickness of 15 nm, except for Mg which was 100 nm. The Alq_3 layer thickness varied from 25 to 150 nm. The Alq_3 layers were sublimed from commercial source materials (sublimed-grade, >99% pure, supplied by H. W. Sands Corp.) at a constant rate of 0.10 nm/s. We also deposited from Alq_3 source materials which had been purified in-house by at least three cycles of entrainment sublimation and found no difference. During the organic deposition, the crucible temperature was monitored and did not vary by more than 1 °C. The electrodes were deposited by thermal evaporation, or for the CoO/Co bottom electrodes, by sputtering. The

deposition rates were kept low at 0.01–0.05 nm/s. In the case of sputtering, low Ar pressure (<1 mTorr) and collimating slits were used to maintain the definition of the shadow masks. The AlO_x tunnel barrier was formed by *in situ* plasma-assisted oxidation of a 1.5-nm evaporated Al layer. To minimize thermal damage to the organic layer from deposition of the top electrode, the metal evaporators were thermally shielded and the substrate was thermally anchored to a sample holder maintained at room temperature. The substrate temperature excursion during top electrode deposition was ~0.5 °C.

Upon completion, we attached leads to the devices in an Ar-filled glove-bag and then loaded them into a Quantum Design Physical Properties Measurement System (PPMS) for measurements. During measurements the samples were sealed in a low-pressure He atmosphere. Since the samples were not encapsulated, we took care to minimize air and moisture exposure during transfers between the deposition system load-lock, the glove-bag, and the PPMS. The yield, defined as the ratio of nonshorted to the total number of devices tested in each set, varied depending on the device size and the Alq_3 layer thickness. Except for those containing the AlO_x barrier layer, all devices with an Alq_3 layer thinner than 50 nm were shorted. For the 100×100 μm^2 devices, the yield was 70% if the Alq_3 layer was 50 nm thick, and was 100% when the Alq_3 layer was 100 nm or thicker. We discarded any set whose yield was less than 70%. Interestingly, all devices containing the AlO_x barrier layer had >70% yield even when the Alq_3 layer was as thin as 25 nm. This is probably due to the improved adhesion of Alq_3 when it is deposited onto an oxide layer.[23]

Because the impedance of the organic junction is many orders of magnitude larger than the lead resistance, the transport measurements were carried out in a two-lead configuration with a Keithley 2400 source meter, at temperatures ranging from 5 to 295 K. For the *J-V* measurements, the bias voltage (V_{bias}), defined as the voltage difference between the anode and cathode, was ramped stepwise and the current was measured in the steady state. Since the difference in the electrode work functions leads to a built-in voltage (V_{bi}) across the organic layer at zero bias, the actual voltage drop across the organic layer (V) is given by $V=V_{bias}-V_{bi}$.

For the MR measurements, the magnetic field was applied in the sample plane and parallel to one of the electrodes. We also measured the anisotropic magnetoresistance of the magnetic electrodes, from which the magnetic configuration of the spin valves was determined.

Using the same fabrication condition for the spin valve structures, we fabricated Alq_3-based OLEDs and magnetic tunnel junctions as control devices. Shown in the inset of Fig. 2(a) is a photograph of two ITO/α-NPD(50 nm)/Alq_3(50 nm)/Al OLED devices operating at a V_{bias} of 5 V. Here ITO is the transparent indium-tin-oxide hole injector, and α-NPD is the N,N′-Di-[(1-naphthyl)-N,N′-diphenyl]-1,1′-biphenyl-4,4′-diamine hole transporting layer. The device exhibits uniform electroluminescence with a turn-on voltage of ~4.5 V. The *J*-V_{bias} curve shows diode behavior, with a current density level typical of this type of OLED. Figure 2(b) shows the MR of a Co/AlO_x/Fe tunnel junction

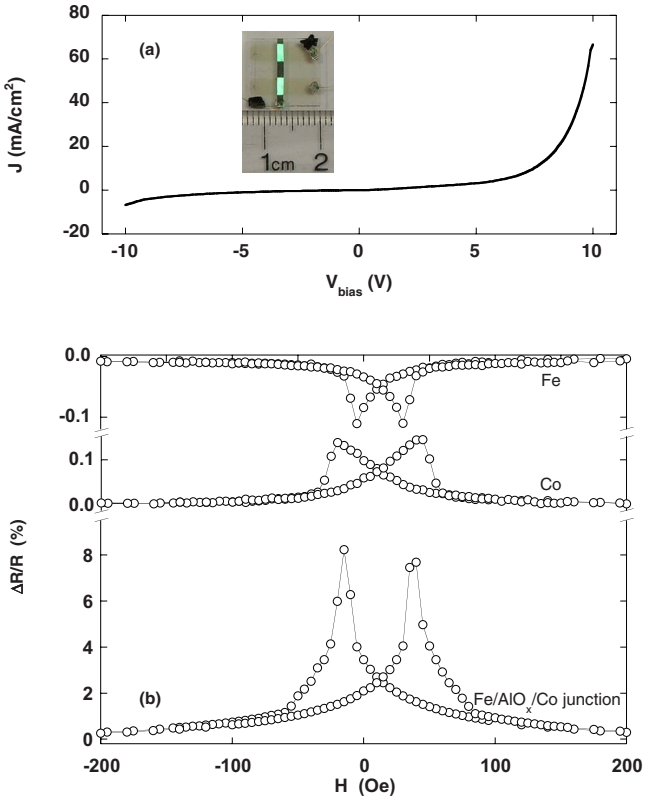

FIG. 2. (Color online) (a) The current density J as a function of the bias voltage V_{bias} for an ITO/α-NPD(50 nm)/Alq_3(50 nm)/Al OLED device. The inset is a photograph of the OLEDs operating at 5 V. (b) Room-temperature magnetoresistance of the Fe and Co electrodes and of the Fe/AlO_x/Co magnetic tunnel junction as a function of the applied magnetic field.

and the Co and Fe electrodes measured at room temperature. At a bias of 50 mV, the TMR of the junction is about 8.5% and the resistance-area (RA) product is 2.3 $\Omega\,cm^2$, both are comparable with literature values. The presence of electroluminescence and TMR effects in the control devices confirms that the growth conditions we adopt can produce good-quality organic layers, and that the magnetic electrodes have appropriate spin polarization and switching properties.

III. RESULTS AND DISCUSSION

We fabricated Co/Alq_3/Fe organic spin valve structures having 50- and 100-nm-thick Alq_3 spacers. Shown in Fig. 3(a) is J measured at 5 K as a function of V_{bias} for a spin valve with a 50-nm Alq_3 spacer. The polarity is defined such that V_{bias} is positive when Co is the anode. The junction is much more conductive at $V_{bias}>0$, resulting in a very asymmetric *J*-V_{bias} curve. This result contrasts with all earlier studies on organic spin valves, where such plots, when shown, are always symmetric.[8,9,15,16] The work functions of Co and Fe are 5 and 4.5 V, respectively,[19] leading to a V_{bi} of 0.5 V. In the inset of Fig. 3(a) we plot *J*-*V* on a log-log scale for the positive and negative polarities. For two orders of magnitude in J (between 10^{-5} and 10^{-7} A/cm^2), the *J*-*V* data for both polarities follow a power law relationship, i.e., J

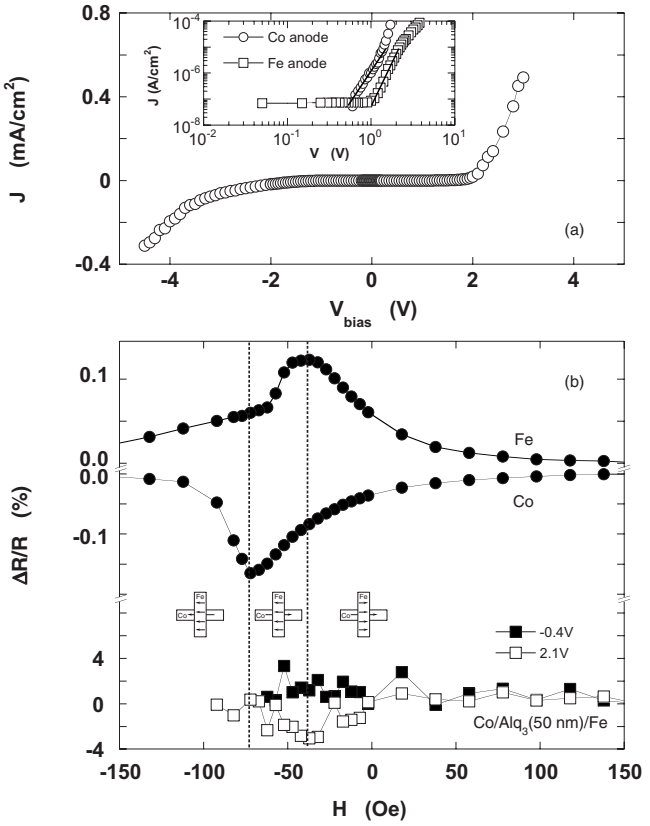

FIG. 3. (a) The current density J as a function of the bias voltage V_{bias} for a Co/Alq_3(50 nm)/Fe device measured at 5 K. Inset: the same data plotted on a log-log scale. The circle and square symbols are for the polarities where Co and Fe are the anodes, respectively. (b) Magnetoresistance at 5 K of the Fe and Co electrodes and of the Fe/Alq_3/Co spin-valve device as a function of the applied magnetic field. The dotted lines mark the magnetic switching of the Fe and Co layers, and the diagrams illustrate the magnetic configurations of the device. The closed and open symbols are for bias levels of −0.4 and 2.1 V, respectively.

$\propto V^m$, as represented by the lines in the log-log plot. The MR of the Fe and Co electrodes and the spin valve measured at 5 K is plotted in Fig. 3(b) as a function of the applied magnetic field. For clarity, only the positive-to-negative field sweep branches are shown. The two dotted lines at 37 and 70 Oe mark the fields at which the Fe and Co electrodes reverse their magnetization directions, respectively. As illustrated by the diagrams, the magnetic configuration of the spin-valve structure switches between being parallel and antiparallel at these two fields. However, when measured at two bias levels (−0.4 and 2.1 V), the spin valve did not show any MR above the noise level. We did not observe any measurable MR effect in all other samples, at any temperature or at any bias.

We note that at current density levels larger than ~1 mA/cm^2, the Fe/Alq_3/Co devices were unstable, often shorting out or becoming open-circuited within hours. However, when the measurement current density was kept lower than 0.1 mA/cm^2, the devices could last for days with reproducible J-V characteristics. We note that the organic spin valves operating in tunneling mode appear able to sustain

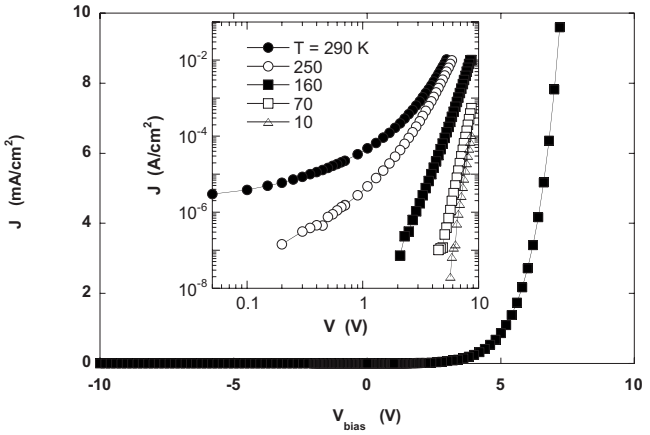

FIG. 4. The current density J as a function of the bias voltage V_{bias} measured at 290 K for a Co/Alq_3(50 nm)/Mg device. Inset: The J-V curves at different temperatures plotted on a log-log scale for the polarity where Mg is the cathode.

significantly higher current densities (~10 mA/cm^2) with no ill-effect.[15,16]

In inorganic semiconductors, spin injection and detection using metallic ferromagnetic contacts have been difficult to ascertain.[12,13] Schmidt *et al.*[18] showed that efficient spin injection by electrical means from ferromagnetic metals into semiconductors is limited by the large mismatch between the conductivities of metals and semiconductors. Ruden and Smith[24] also theoretically modeled electrical spin injection from a metallic ferromagnetic contact into an organic semiconductor and concluded that the electron distribution cannot be driven far from thermal equilibrium by practical current densities. The typical metal resistivity is just a few $\mu\Omega$ cm. By comparison, Alq_3 has a resistivity of at least 1.2 mΩ cm for electron transport even when the conduction is in the space-charge-limited regime.[25] The electron mobility in Alq_3 is about two orders of magnitude higher than the hole mobility,[26] meaning that Alq_3 resistivity is even higher when holes are being transported. Therefore spin injection into Alq_3 from Fe and Co electrodes faces the same "conductivity mismatch problem," and a magnetoresistance effect in Fe/Alq_3/Co spin valve devices is not expected.

In order to shed light on the discrepancy between our null MR result and the earlier reports of GMR and TMR in Alq_3-based spin valve devices, we examine the nature of the charge transport in Alq_3 from Co and Fe electrodes using unipolar devices. Shown in Fig. 4 is J measured as a function of V_{bias} for a Co/Alq_3(50 nm)/Mg device at 290 K. Positive V_{bias} denotes when Co is the anode and Mg is the cathode. J is near zero when $V_{\text{bias}}<0$. Because Mg is an electron-injecting material, the absence of conduction at $V_{\text{bias}}<0$ means that the Co cathode cannot inject electrons into Alq_3. This is reasonable considering that the energy barrier for electron injection from Co is ~2.8 eV (see Fig. 1). At $V_{\text{bias}}>0$, conduction occurs and J rises rapidly when $V_{\text{bias}}>1$ V. This is the case where electrons may be injected from Mg and holes may be injected from Co. However, since the energy barrier for electron injection from Mg is ~1.46 eV and the barrier for hole injection from Co is ~1.8 eV, the elec-

tron current is expected to dominate. Indeed, the J-V curves from several different temperatures as shown in the inset are very similar to those of electron-only injection from Mg into Alq_3.[22] The J-V curves again follow a power law relationship ($J \propto V^m$); the exponent m increases with decreasing temperature but becomes nearly constant at low temperatures. Such behavior is due to the distribution of interfacial sites to and from which the electrons hop.[22] Although it may seem possible for an Fe cathode to inject electrons given that the energy barriers for electron and hole injection from Fe are both ~2.3 eV, this barrier is higher than that for hole injection from Co. Transport in $Fe/Alq_3/Co$ spin valve devices is therefore by holes only. This conclusion is supported by our observation that these devices are stable only at low current densities. The different slopes of the lines in Fig. 3(a) inset reflect the difference in the hole injection barrier from Co and Fe electrodes.

That the charge transport in $Fe/Alq_3/Co$ spin valves is *hole-only* has important ramifications. It has been shown that unbalanced hole transport in Alq_3 leads to unstable cationic species and is the main cause of degradation of OLED devices.[27] This degradation mechanism explains the need to limit current density in our $Fe/Alq_3/Co$ spin valves, and may also be related to the reported failure and intensity drift in OLEDs with ferromagnetic electrodes.[6,14] The degradation of Alq_3 by a hole current presents a difficulty with attributing the MR in Alq_3 spin valves to the GMR effect, as was done in Refs. 8–10. Because the metal electrodes (Fe, Co, Ni, and $La_{0.67}Sr_{0.33}MnO_3$) all have high work function and would inject holes, which then drift through the Alq_3 layer in the GMR process, a large hole current such as that used in Ref. 10 (>1 mA/cm^2) would have resulted in unstable devices. On the other hand, for spin valves operating in tunneling mode, such as those in Refs. 15 and 16 where the Alq_3 is ultrathin, the tunneling charge carriers have, by definition, lower energy than the barrier and thus do not occupy the molecular levels. Since the oxidative reaction may not occur, high current densities may be sustained in those Alq_3 tunnel junctions.

The current density used in Refs. 8 and 9 is sufficiently low (<0.1 mA/cm^2) so that the hole transport does not cause Alq_3 degradation. However, the lack of MR in our spin valves is at variance with the report of GMR in similar structures in Ref. 9. To verify that the characteristics of our samples are what is expected of hole transport in well-formed Alq_3 layers and Alq_3-metal interfaces, we present the temperature-dependent transport properties of unipolar $Co/Alq_3/Au$ structures measured at low current densities, and compare them with modeling results obtained from using the nominal Alq_3 thicknesses and an injection barrier value typical of well-formed Alq_3-metal interfaces.

Depending on the height of the charge injection barrier, the current in organic devices is either transport-limited or injection-limited. These situations can be distinguished from the characteristic dependence of current density J on the electric field E and the organic thickness d. The transport-limited case gives $J \propto E^{m+1}/d^m$, whereas if the current is injection-limited, the $J(E)$ curves do not depend on d.[28] In Fig. 5(a) we plot the $J(E)$ curves of two $Co/Alq_3/Au$ hole-only devices measured at several temperatures, for the polarity where holes are being injected from the Co anode. The thicknesses of the Alq_3 layers in these devices are 50 and 100 nm, respectively. At high temperatures, the data sets for the two samples overlap, i.e., the current density depends only on the electric field, not the Alq_3 thickness. Thus hole transport from Co to Alq_3 is injection-limited at high temperatures. In Fig. 5(b), we plot the power law exponent m extracted for the $J(E)$ data as a function of temperature. The exponent increases very slowly with decreasing temperature, varying from 1.5 at 290 K to 3 at 10 K. This weak temperature dependence suggests a distribution in the energy of the interfacial sites where the holes can hop to and from. We calculated m using the charge-injection model of Arkhipov *et al.*,[28] assuming an injection barrier of 1.8 eV and an energy distribution of 0.4 eV for the interfacial sites. The agreement at high temperatures is quite good. This suggests that the Alq_3 layers in our samples are free from metal inclusions and that the Alq_3-metal interfaces are well-formed. At low temperatures, the measured m is much lower than the calculated values. This could be due to the reduced hole mobility at the lower temperatures,[26] where the current becomes transport limited and the injection model is no longer applicable.

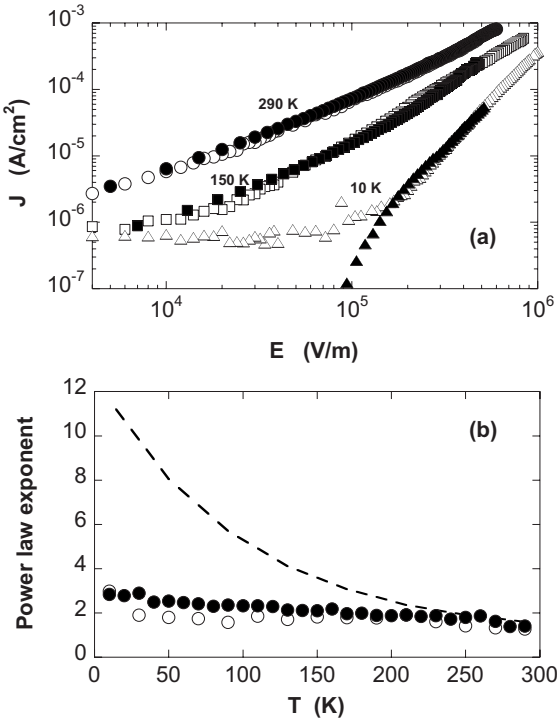

FIG. 5. (a) Current density J as a function of the electric field E measured at different temperatures for two hole-only devices: Co/Alq_3(50 nm)/Au (open symbols) and Co/Alq_3(100 nm)/Au (closed symbols). (b) The temperature dependence of the power law exponent for the Co/Alq_3(50 nm)/Au (open circles) and Co/Alq_3(100 nm)/Au (closed circles) hole-injection-only devices. The dashed curve is from model calculations for an injection barrier of 1.8 eV and an energy distribution of 0.4 eV for interfacial sites.

The difficulty in spin injection from ferromagnetic metals into semiconductors can be circumvented by introducing an injection barrier.[29,30] Ruden and Smith proposed the same for spin injection at the metal-organic interface.[24] The role of the

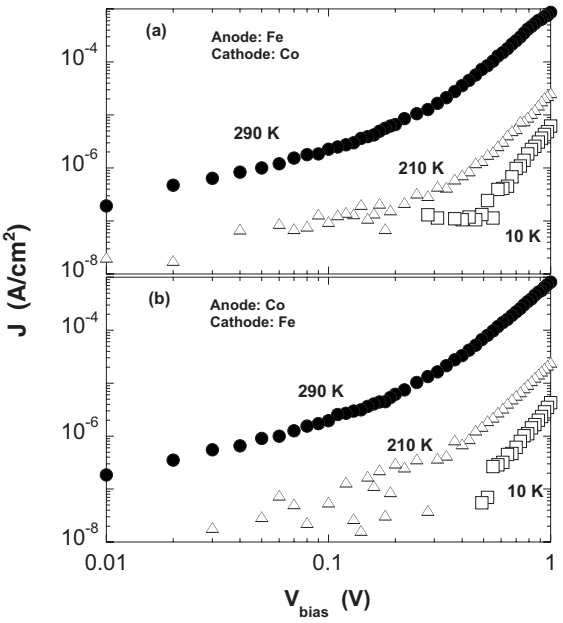

FIG. 6. Current density as a function of voltage difference measured at different temperatures for a $Co/AlO_x/Alq_3(25\ nm)/Fe$ device.

injection barrier is to drive the semiconductor out of local thermal equilibrium and promote spin accumulation. We inserted an AlO_x tunnel barrier between the ferromagnetic electrode and the Alq_3 layer, but detected no measurable MR. The insertion of the tunnel barrier did change the transport characteristics, however. Shown in Fig. 6 are the J-V_{bias} curves for a $Co/AlO_x/Alq_3(25\ nm)/Fe$ device measured at different temperatures. The J-V_{bias} curves are now symmetric with respect to bias polarity. It appears that the AlO_x tunnel barrier may have adjusted the vacuum level offset in a way that equalizes the hole injection barriers for the Fe and Co electrodes, making them equally capable of injecting holes into Alq_3. Since the spin-polarized holes exiting the tunnel barrier are not at equilibrium with the molecular level, i.e., the interfacial impediment to spin injection is removed, the absence of MR in this case hints at other intrinsic mechanisms that might depolarize the spin current during hole transport in Alq_3.

IV. CONCLUSION

We have fabricated and measured the transport properties of Alq_3-based spin valves and unipolar devices where the Alq_3 thickness is larger than the tunneling limit. We observe no measurable magnetoresistance in our $Fe/Alq_3/Co$ spin valve structures. By comparing with the temperature-dependent current density-voltage characteristics of unipolar devices, we show that charge transport in $Fe/Alq_3/Co$ spin valves is by holes only; the hole-only transport in Alq_3 is stable only at low current densities and is injection-limited. That the hole-only transport in $Fe/Alq_3/Co$ spin valves cannot support the high current densities as used in earlier studies supports the interpretation of tunneling as the mechanism for the magnetoresistance in those reports. The lack of magnetoresistance in $Fe/Alq_3/Co$ spin valve is similar to the case of a ferromagnetic metal-inorganic semiconductor interface, where the "conductivity mismatch problem" prevents efficient spin injection. However, inserting a tunnel barrier between the magnetic electrode and the organic semiconductor did not improve spin injection. This suggests possible intrinsic spin-depolarizing hole transport in Alq_3.

ACKNOWLEDGMENT

Work supported by U.S. Department of Energy Office of Science Basic Energy Sciences, under Contract No. DE-AC02-06CH11357.

[1] S. A. Wolf, D. D. Awschalom, R. A. Buhrman, J. M. Daughton, S. von Molnár, M. L. Roukes, A. Y. Chtchelkanova, and D. M. Treger, Science **294**, 1488 (2001).
[2] V. I. Krinichnyi, Synth. Met. **108**, 173 (2000).
[3] M. Ouyang and D. D. Awschalom, Science **301**, 1074 (2003).
[4] J. R. Petta, S. K. Slater, and D. C. Ralph, Phys. Rev. Lett. **93**, 136601 (2004).
[5] S. R. Forrest, Nature (London) **428**, 911 (2004).
[6] A. H. Davis and K. Bussmann, J. Appl. Phys. **93**, 7358 (2003).
[7] V. Dediu, M. Murgia, F. C. Matacotta, C. Taliani, and S. Barbanera, Solid State Commun. **122**, 181 (2002).
[8] Z. H. Xiong, D. Wu, Z. V. Vardeny, and J. Shi, Nature (London) **427**, 821 (2004).
[9] F. J. Wang, Z. H. Xiong, D. Wu, J. Shi, and Z. V. Vardeny, Synth. Met. **155**, 172 (2005).
[10] S. Pramanik, S. Bandyopadhyay, K. Garre, and M. Cahay, Phys. Rev. B **74**, 235329 (2006).
[11] S. Majumdar, H. S. Majumdar, R. Laiho, and R. Österbacka, J. Alloys Compd. **423**, 169 (2006).
[12] W. Y. Lee, S. Gardelis, B. C. Choi, Y. B. Xu, C. G. Smith, C. H. W. Barnes, D. A. Ritchie, E. H. Linfield, and J. A. C. Bland, J. Appl. Phys. **85**, 6682 (1999).
[13] P. R. Hammar, B. R. Bennett, M. J. Yang, and M. Johnson, Phys. Rev. Lett. **83**, 203 (1999); F. G. Monzon, H. X. Tang, and M. L. Roukes, *ibid.* **84**, 5022 (2000); B. J. van Wees, *ibid.* **84**, 5023 (2000); P. R. Hammar, B. R. Bennett, M. J. Yang, and M. Johnson, *ibid.* **84**, 5024 (2000).
[14] G. Salis, S. F. Alvarado, M. Tschudy, T. Brunschwiler, and R. Allenspach, Phys. Rev. B **70**, 085203 (2004).
[15] W. Xu, G. J. Szulczewski, P. LeClair, I. Navarrete, R. Schad, G. Miao, H. Guo, and A. Gupta, Appl. Phys. Lett. **90**, 072506 (2007).
[16] T. S. Santos, J. S. Lee, P. Migdal, I. C. Lekshmi, B. Satpati, and J. S. Moodera, Phys. Rev. Lett. **98**, 016601 (2007).
[17] J. C. Scott, J. Vac. Sci. Technol. A **21**, 521 (2003), and references therein.
[18] G. Schmidt, D. Ferrand, L. W. Molenkamp, A. T. Filip, and B. J. van Wees, Phys. Rev. B **62**, R4790 (2000).

[19] H. B. Michaelson, J. Appl. Phys. **48**, 4729 (1977).
[20] I. G. Hill, A. Kahn, Z. G. Soos, and R. A. Pascal, Chem. Phys. Lett. **327**, 181 (2000).
[21] H. Ishii, K. Sugiyama, E. Ito, and K. Seki, Adv. Mater. (Weinheim, Ger.) **11**, 605 (1999).
[22] M. A. Baldo and S. R. Forrest, Phys. Rev. B **64**, 085201 (2001).
[23] H. W. Choi, S. Y. Kim, W. Kim, K. Hong, and J. Lee, J. Appl. Phys. **100**, 064106 (2006).
[24] P. P. Ruden and D. L. Smith, J. Appl. Phys. **95**, 4898 (2004).
[25] M. Stößel, J. Staudigel, F. Steuber, J. Blässing, and J. Simmerer, Appl. Phys. Lett. **76**, 115 (2000).
[26] R. G. Kepler, P. M. Beeson, S. J. Jacobs, R. A. Anderson, M. B. Sinclair, V. S. Valencia, and P. A. Cahill, Appl. Phys. Lett. **66**, 3618 (1995).
[27] H. Aziz, Z. D. Popvic, N. Hiu, A. Hor, and G. Xu, Science **283**, 1900 (1999).
[28] V. I. Arkhipov, E. V. Emelianova, Y. H. Tak, and H. Bassler, J. Appl. Phys. **84**, 848 (1998).
[29] E. I. Rashba, Phys. Rev. B **62**, R16267 (2000).
[30] A. Fert and H. Jaffres, Phys. Rev. B **64**, 184420 (2001).